Chapter 3

QUANTUM WELL LASERS

3.1 Introduction

When light is confined into a cavity smaller than its wavelength, it behaves as a particle rather than as a wave. Then an entirely new class of physical phenomena, called quantum size effect appears. In the case of semiconductor lasers, quantum behavior changes the operation of the laser in a dramatic and fundamental way.

Most semiconductor lasers are very thin (~20 microns) in the vertical direction but this is not thin enough to cause quantum behavior. In QW lasers, layer thickness (cavity height) is reduced to around 10 to 20 nm. The most obvious change in laser characteristic that this brings is that the amount of material in the region is substantially reduced. This reduces the amount of energy needed to achieve lasing and thus the lasing threshold, resulting a higher gain characteristic but a lower maximum output power. In addition, quantum wells have a much lower sensitivity to temperature change. In the very thin layer available, there is much less space for energy and momentum effects to occur. The quantum well structure prevents lateral modes forming and ensures that lasing produces only one line. In addition the linewidth of single line produced is narrower than for non-QW structures.

Lasers with a single active region are called "Single Quantum Well" (SQW) lasers. Normally a number of quantum wells are used one on top of

another. These are called "Multiple Quantum Well" (MQW) structures. MQW structures retain many of the desirable characteristics of SQW but produce a higher gain and greater total power. A disadvantage is that MQW lasers produce a broader linewidth than SQW but still narrower than comparable non-QW structures.

3.2 Quantum Well Layer

A heterostructure QW is a thin layer of narrower band gap semiconductor sandwiched between two thicker layers of wider band gap semiconductor. Thin layer means that the thickness of the layer is less than a few hundreds of Angstroms. A double heterojunction structure with the band diagramme is schematically shown in Figure 3.1.

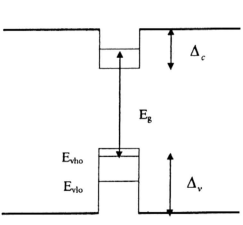

Figure 3.1 *Energy band diagramme of a nominal quantum well*

The narrower band gap layer is seen as a potential well for both electrons and holes. If it is thinner than the characteristic carrier free path, motion of those

carries along the growth axis is quantized and hence is a quantum potential well (QW). A QW layer can contain one or more QWs, and itself is a multi-layer heteroepitaxial structure. The quantum wells always are considered to be square-shape and isolated, with the barrier heights modified due to the exchange-correlation interaction and strain effects as described in section 3.6.2.

3.3 Strained Layer Quantum Wells

Semiconductor lasers had been made from lattice matched heterostructures, such as GaAs/AlGaAs and InGaAsP/InP. This situation changed rapidly when an important new development in quantum well lasers occurred since early 1980's with the use of strained quantum wells. The driving force behind this advancement has been the development of thin film epitaxy technique such as *Molecular Beam Epitaxy* (MBE) and *Metal-organic Chemical Vapour Deposition* (MOCVD).

For lattice matched structure, the crystalline structure of the material must be continuous across the junction. This means that the crystal lattices of the different types of material on each side must join into a single crystal. If the spacing of the atoms in the different materials is too different then interfacial misfit dislocation occurs in the crystal structure around the junction, destroying the operation of the laser diode. The presence of the crystal defects can severely degrade the optical and electronic properties of heterostructures. To avoid misfit dislocation, only lattice matched semiconductor or with lattice mismatch much less than 1% were chosen in the fabrication of heterostructure devices.

Strained layer heterostructure can be formed by sandwiching an extremely thin (~ 2 nm) semiconductor layer between much thicker layers of a material with a significantly different lattice constant. A large strain is built into the epitaxial layer while still maintaining good crystalline quality. The atoms in the thin layer are pulled apart (tensile strain) or forced together (compressive strain) to conform to the crystalline structure of the surrounding material. This means that the chemical bonds holding the material together become longer or shorter than their natural length. The atoms of the thin material layer conform to the lattice structure of the thicker layers without misfit dislocation or cracking.

This results in two very beneficial effects.

a) It allows the use of a much wider range of material in the heterojunction. Strained layer epitaxy provides more material choices than lattice matched layer epitaxy. This additional freedom makes strained layer heterostructure an attractive candidate for semiconductor device applications. Strained layer quantum wells can be used to generate laser emission at new wavelengths.

b) The strain in the lattice of the thinner layer changes its properties in a number of highly desirable ways. Most obviously, it changes the band gap energy levels. By engineering the amount of strain, the band gap (laser wavelength) can be tuned without affecting too much the semiconductor properties of the junction. In addition, the strain allows the device to operate at significantly lower threshold currents than are possible in unstrained MQW lasers.

3.4 Structural Aspects of Strained Layers

Consider a material InGaAs is grown on GaAs with a different lattice constant. InGaAs has larger lattice constant than GaAs as shown in Figure 3.2(a) in equilibrium.

The GaAs substrate is so thick that it cannot be distorted significantly. However, the thin layer of InGaAs can strain to conform to the GaAs in the plane of the junction as in Figure 3.2(b). In this case, the lattice constant of InGaAs in the plane is reduced to that of GaAs, while the usual elastic response causes InGaAs to extend along the direction of growth. Thus InGaAs is distorted severely and enormous elastic energy builds up. Only the thin film can tolerate such stress. In a thick film, relaxation occurs and the InGaAs takes up its natural lattice constant. Consequently, perfect matching of the atoms at the heterojunction no longer exists. Instead the difference in lattice constants is taken up by misfit dislocation and many bonds are broken, as shown in Figure 3.2(c).

The elastic energy of a strained layer is roughly proportional to its thickness. There is therefore a critical thickness beyond which it costs too much energy to strain additional layers into coherence with the substrate and dislocation appears. Matthews-Blakeslee criterion calculated the critical thickness of a layer by considering the strain and the lattice constant.

The defects associated with a relaxed layer are not localized only in the plane of the interface. The dislocations may turn upwards and become threading dislocations which terminate on the exposed surface of the sample. It will be damaging when they pass through the active region. Thus thick relaxed buffer layers are grown so that cheap and readily available substrates (GaAs) can be used under materials of different lattice constant.

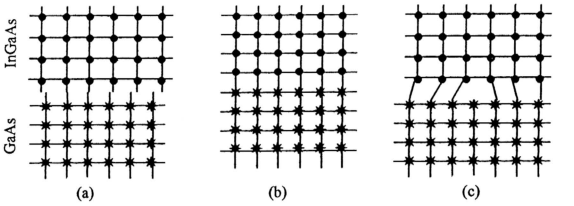

Figure 3.2 Growth of InGaAs on GaAs substrate.
(a) Separate layers at equilibrium.
(b) Thin layer of InGaAs on GaAs, the lattice constants are conforming.
(c) Thicker layer of InGaAs, where misfit dislocation occur.

3.5 Band Structure Under Strain

The most obvious effect of strain is to move the edges of the bands. This is essential in the indirect stimulated transitions. Strain has more dramatic effects on the degenerate valence band near Γ and opens another important route to band engineering.

Figure 3.3 shows the effect of strain on the bands of a semiconductor layer. The valance band is split and the band gap is much reduced. In Figure 3.3(a), the active layer has a smaller lattice constant and tension is applied in the plane. The effect of compression of the lattice in the plane of the junction is illustrated in Figure 3.3(c) where the active layer has larger lattice constant. The active layer is unstrained in Figure 3.3(b), showing the usual band structure. The material composition and strain in a QW are not the independent parameters. In

the case of the quaternary compounds $Ga_xIn_{1-x}As_yP_{1-y}$, the QW strain parameter is interconnected with the mole fraction x and y by[4]

$$\delta = \frac{0.0125xy - 0.4176x + 0.1896y}{5.8688 \times 10^{-2}} \quad (\%) \qquad (3.5.1)$$

where δ is the QW strain expressed in %. Tensile strain is valued positively while compressive strain is negative.

The bands in a strained quantum well are affected both by the strain and by the confinement. They reduce the symmetry in the same way and pull the top valence bands further apart. Thus a larger density of holes can be accommodated in the top valence band alone before the next band is also populated. As a result, by using strained quantum wells, the performance of semiconductor lasers has been improved substantially.

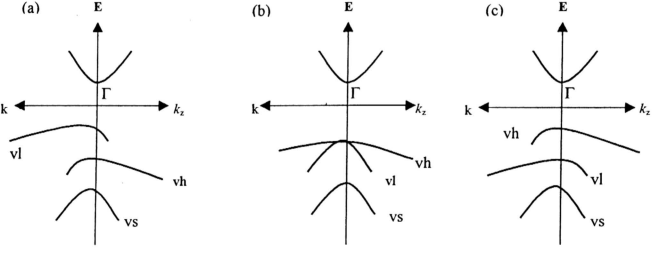

Figure 3.3 Effect of strain on the bands of a semiconductor, showing the splitting of valence band.

(a) The effect of tension of the lattice in the plane of the junction.
(b) The layer is unstrained.
(c) The effect of compression of the lattice in the plane of the junction.

vh: heavy hole valance band
vl; light hole valance band
vs: split-off valence band

3.6 Theory of Quantum Well Layer

The general approaches applied in the modeling of optical design and characterization in bulk layer of semiconductor lasers extended to the QW and furthermore strained QW structure. In QW layer, the potential well is thinner than the characteristic carrier mean free path. The carrier energy in such a well is quantized, acquiring only a finite number of discrete values of energy level, termed quantum subbands. All electrons and holes may be trapped in the lowest level. Motion parallel to the layers is not affected. This result is a two-dimensional (2D) carrier state. In the barrier, the motion of the carriers behave as those in the real three-dimension (3D). The former is known the bound state and the latter is the unbound state. This is an additional feature of QW incorporated in the barrier bulk layer. The optical properties obtained in the bulk layer are applicable in QW layer with certain modifications added on the model due to the size quantization. The similar procedures will be adopted in analyzing the optical properties of QW layer.

3.6.1 Carrier Distribution

In the QW layers, carriers are injected into unbound states in the barriers while the carriers are trapped into bound states in the potential wells. The wells are considered to be square-shaped and the electrons (holes) with energy above (below) the barriers are treated as bulk-like 3D carriers while those below (above) the barriers are localized 2D carriers. Both the electron and hole Fermi levels are constant across the QW layer, thus the layer is electrically neutral. The Fermi-

Dirac functions give the quasi-equilibrium occupation probabilities for 3D and 2D subbands in conduction or valence band,

$$f_i(\varepsilon_i) = \left\langle 1 + \exp\left[\frac{\varepsilon_i}{T_i} - \xi_i(z)\right]\right\rangle^{-1} \qquad i = c, v \tag{3.6.1}$$

Here, $\xi_i(z)$ is the normalized chemical potential, ε_i is the energy relative to the band edges which is defined as follows:

$$\varepsilon_i(k) = E_i + \varepsilon_{ik} \tag{3.6.2}$$

where E_i is the quantum subband edge, while ε_{ik} is the kinetic energy associated with the motion in the plane of QW, related to the in-plane effective mass in the well, $m_{i\perp w}$.

$$\varepsilon_{ik} = \frac{\hbar^2 k^2}{2m_{i\perp w}} \tag{3.6.3}$$

As in the bulk layer, the Fermi levels in conduction and valence bands, Φ_c and Φ_v, are resolved from the total sheet concentrations of electrons and holes in QW layer, $N_{c,s}$ and $N_{v,s}$. These involve the integral over the 3D and 2D subbands,

$$N_{i,s} = \sum_{(wells)} N_{i,2D} + \int_{(barriers)} dz N_{i,3D}(z) \qquad i = c, v \tag{3.6.4}$$

The $N_{i,3D}$ is determined as the bulk concentration in equation (3.5.7). The sheet concentration of 2D carriers is given by

$$N_{i,2D} = \sum_{(J)} \aleph_{ij,2D}(T_i) \ln\left[1 + \exp\left(\xi_{iw} - \frac{E_{ij}}{T_i}\right)\right] \tag{3.6.5}$$

Here, the 2D density of states at the subband edge,

$$\aleph_{ij,2D}(T_i) = 2\left[\frac{2\pi m_{ij\perp w} T_i}{(2\pi\hbar)^2}\right] = \frac{m_{ij\perp w} T_i}{\pi\hbar^2} \tag{3.6.6}$$

The above result is obtained assuming that the wells are square-shaped. When the band bending is taken into account, the effective concentration is calculated as

$$N_{i,2D} = \sum_{(j)} \aleph_{ij,2D}(T_i) \int_{E_{ij}/T_i}^{\varepsilon_{ij\max}/T_i} \frac{du \rho_{ij}(u)\Gamma_{ij}(u)}{1+\exp(u-\xi_{iw})} \tag{3.6.7}$$

with ξ_{iw} denotes the normalized chemical potential in the well and the reduced density of states in 2D subband is given by

$$\rho_{ij}(k) \equiv \frac{d\varepsilon_{ik}}{d\varepsilon_i(k)} = \left\{1-(1-\zeta_{i\perp})\left[1+\zeta_{iz}\frac{q_{ijb}^2(k)}{q_{ijw}^2(k)}+q_{ijb}(k)\left(1+\zeta_{iz}^2\frac{q_{ijb}^2(k)}{q_{ijw}^2(k)}\right)\right]^{-1}\right\}^{-1} \tag{3.6.8}$$

Γ_{ij} is the quantum confinement factor given by

$$\Gamma_{ij}(k) = \left\langle 1+\zeta_{iz}\frac{q_{ijb}(k)}{q_{ijw}^2(k)}\left[1+\zeta_{iz}\frac{q_{ijb}^2(k)}{q_{ijw}^2(k)}\right]^{-1}\right\rangle \left\langle 1+\frac{1}{q_{ijb}(k)}\left[1+\zeta_{iz}\frac{q_{ijb}^2(k)}{q_{ijw}^2(k)}\right]\left[1+\zeta_{iz}^2\frac{q_{ijb}^2(k)}{q_{ijw}^2(k)}\right]^{-1}\right\rangle^{-1} \tag{3.6.9}$$

where q_{iw} and q_{ib} are the parameters defined as

$$q_{iw} = \frac{d_w}{\hbar}\sqrt{2m_{izw}(\varepsilon_i-\varepsilon_{ik})} \tag{3.6.10}$$

$$q_{ib} = \frac{d_w}{\hbar}\sqrt{2m_{izb}(\Delta_i-\varepsilon_i+\zeta_{i\perp}\varepsilon_{ik})} \tag{3.6.11}$$

and the well-to-barrier in-plane effective mass ratios are expressed by

$$\zeta_{i\perp} = \frac{m_{i\perp w}}{m_{i\perp b}} \tag{3.6.12}$$

3.6.2 Strain and Band Gap Shrinkage Effects

As mentioned in section 3.5, the lattice mismatch between the epitaxial layers and substrate induces strain in QW layer. This induced strain changes the band gap energy levels and causes band edge shift. The shift of the band edge $\Delta_{i,str}$ is proportional to the relative change in the lattice constant δ. From the Pikus-Bir Hamiltonian, the shift of the band edge for the conduction, heavy hole and light hole bands can be expressed as

$$\Delta_{c,str} = 2A_c(1 - C_{12}/C_{11})\delta \tag{3.6.13}$$

$$\Delta_{vh,str} = -[2A_v + B - 2(A_v - B)C_{12}/C_{11}]\delta \tag{3.6.14}$$

$$\Delta_{vl,str} = -[2A_v - B - 2(A_v + B)C_{12}/C_{11}]\delta \tag{3.6.15}$$

where A_c, A_v and B are the deformation potentials for the conduction and valence bands, C_{11} and C_{12} are the elastic constants. All these parameters are defined in Appendix 1.

As in the bulk layer, the band gap shrinkage in QW is caused by the exchange-correlation interaction of free carriers. The conduction band edge is shifted up while the valence band edges are shifted down, causing an increase in the barrier height. This shift is calculated as

$$\Delta_{i,xc}(N_{i,eff}) = 0.0582\{1 + 0.7734\eta_i^{-1}(N_{i,eff})\ln[1 + \eta_i(N_{i,eff})]\}\eta_i(N_{i,eff})R_i \tag{3.6.16}$$

Thus, with the contribution of strain and band gap shrinkage, the barrier height becomes

$$\Delta_i = \Delta E_i + \Delta_{i,str} + \Delta_{i,xc} \tag{3.6.17}$$

where ΔE_i is the band offset at heterojuction in a nominal QW.

3.6.3 Complex Permittivity from 2D Subbands

Both the imaginary and real parts of the effective permittivity are calculated similar to those in the bulk layer with an additional contribution from 2D subbands.

The imaginary part of permittivity in QW layer combines those from all the QWs which are considered to be isolated and identical. It is expressed as follows :

$$\kappa''_{\omega,2D} = \frac{v_w}{d}\frac{2\pi e^2 E_p}{3m_o\hbar^2\omega^2}\sum_{(m,n)}\mu_{cvm}\int_0^{\varepsilon_{k,max}} d\varepsilon_k M_{vm}^{cn}(\varepsilon_k)\{1-f_v[\varepsilon_{vm}(\varepsilon_k)]-f_c[\varepsilon_{cn}(\varepsilon_k)]\}\times$$

$$\delta_1[\varepsilon_{vm}(\varepsilon_k)+\varepsilon_{cn}(\varepsilon_k)+E_{gw}-\hbar\omega] \tag{3.6.18}$$

Here, E_{gw} is the band gap in the well, v_w is the number of QW, d is the total width of the layer, $\varepsilon_{vm}, \varepsilon_{cn}$ and $f_c(\varepsilon_{vm}), f_c(\varepsilon_{cn})$ are the energies and occupation probabilities of the participating states, the reduced effective mass of electron-hole pair is defined as

$$\mu_{cvm} = m_{vm\perp w}m_{c\perp w}(m_{vm\perp w}+m_{c\perp w}) \tag{3.6.19}$$

$$\varepsilon_k = \frac{\hbar^2 k^2}{2\mu_{cvm}} \tag{3.6.20}$$

And within a framework of the parabolic subband approximation to the Kane model, the reduced matrix element for TE and TM polarization are

$$M_{vm}^{cn} = \begin{cases} I_{v1m}^{cn} + \frac{1}{3}I_{v2m}^{cn} & TE \\ \frac{4}{3}I_{v2m}^{cn} & TM \end{cases} \tag{3.6.21}$$

where I_{v1m}^{cn} and I_{v2m}^{cn} are the squared overlap integrals of the m-th quantum

subband in the valence band related to the states $|1\rangle$ and $|2\rangle$, respectively. They are expressed in the forms:

$$I_{vjm}^{cn}(k) = d_w A_{cn}(k) A_{vjm}(k) \times$$

$$\left\{ \frac{\sin\left[q_{cnw}(k) - q_{vjmw}(k)\right]}{q_{cnw}(k) - q_{vjmw}(k)} + \frac{\sin\left[q_{cnw}(k) + q_{vjmw}(k)\right]}{q_{cnw}(k) + q_{vjmw}(k)} + 2\frac{\cos\left[q_{cnw}(k)\right]\cos\left[q_{vjmw}(k)\right]}{q_{cnb}(k) + q_{vjmb}(k)} \right\}$$

- even states - (3.6.22)

$$I_{vjm}^{cn}(k) = d_w A_{cn}(k) A_{vjm}(k) \times$$

$$\left\{ \frac{\sin\left[q_{cnw}(k) - q_{vjmw}(k)\right]}{q_{cnw}(k) - q_{vjmw}(k)} + \frac{\sin\left[q_{cnw}(k) + q_{vjmw}(k)\right]}{q_{cnw}(k) + q_{vjmw}(k)} + 2\frac{\cos\left[q_{cnw}(k)\right]\cos\left[q_{vjmw}(k)\right]}{q_{cnb}(k) + q_{vjmb}(k)} \right\}$$

- odd states - (3.6.23)

$$A_{ij}(k) = \frac{1}{\sqrt{d_w}} \left\{ 1 + \frac{1}{q_{ijb}(k)} \left[1 + \zeta_{iz} \frac{q_{ijb}^2(k)}{q_{ijw}^2(k)} \right] \left[1 + \zeta_{iz}^2 \frac{q_{ijb}^2(k)}{q_{ijw}^2(k)} \right]^{-1} \right\}^{-1/2} \quad (3.6.24)$$

For the real part of permittivity, the contribution of the induced anomalous dispersion is determined as[4]

$$\Delta\kappa'_{\omega 2D,ad} = \frac{2}{\pi} PV \int_0^\infty \frac{d\varpi \varpi \kappa''_{\varpi 2D}}{\varpi^2 - \omega^2} \quad (3.6.25)$$

The free carriers in 2D subbands also contribute to the real part of permittivity through dynamic plasma polarization as follows :

$$\Delta\kappa'_{\omega 2D,pl} \cong -\frac{4e^2 \nu_w}{\hbar^2 \omega^2 d} \sum_{(i)} T_i \sum_{(j)} \ln\left[1 + \exp\left(\xi_{iw} - \frac{E_{ij}}{T_i} \right) \right] \quad (3.6.26)$$

Subsequently, the overall contribution of 2D subbands to the real part of permittivity in QW layer is

$$\Delta\kappa'_{\omega 2D} = \Delta\kappa'_{\omega 2D,ad} + \Delta\kappa'_{\omega 2D,pl} \quad (3.6.27)$$